HEAT STORAGE CAPABILITY ON ASYMMETRICALLY COOLED WALL BY TRANSIENT HEAT FLOW

L. Hach 1, Y.Katoh 2

1 Institute of Applied Physics and Mathematics, Faculty of Chemical Engineering,
University of Pardubice, 532 10 Pardubice, Czech Rep.
2 Department of Mechanical Engineering, Faculty of Engineering,
Yamaguchi University, 755 8611 Ube, Japan

Abstract

A strong rationale for energy efficiency and its savings in buildings aims to further develop new concepts as well as more accurate calculation and simulation techniques. In the paper is described efficient implementation of basic relations governing the thermal energy transfer process within the vertical wall into a state-variable model of wall segment with time-dependent properties.

1 Introduction

The heat transfer occurring at building envelopes is one of primary causes of overall heat losses and there are several passive as well as active arrangements to reduce them significantly. While the heat transfer phenomena are always acting in three different kinds of energy transport (conduction, convection and radiation), the energy stored within the envelope's mass is in fact dynamical in nature. This work discusses the way of automated measurement and calculation of main quantities characterizing the time-dependent heat storage amount in building's envelopes parts, i.e. on window plates and outside walls. On the outside-faced wall surface area are measured temperatures via surface temperature sensors, similarly like on the inside-faced wall surfaces. The measurement data set is part of input vector onto a mathematical model which includes beside the envelope's segment adjacent air layers.

With the model were investigated two thermal states: in ‚normalized' state (50 % of air of relative humidity), and with real data measured. Both states were simulated as one-dimensional heat transmission through a concrete wall and as result were obtained dynamic characteristics: overall time constant,

$$\tau_j = \frac{\sum_{j=1}^{n} c_j \rho_j V_j}{h_j A_j} \qquad j = 1,2,...n \qquad (\mathrm{s}) \tag{1}$$

thermal damping (Fig.1) and heat capacity of the wall segment, respectively:

$$\sum_{j=1}^{n} m_j c_j \qquad j = 1,2,...n \qquad \left(\mathrm{J.K^{-1}}\right) \tag{2}$$

Both adjacent segments (gypsum) of the wall, i.e. the ones facing exterior, resp. interior, would satisfy $Bi > 0.1$, as result of a dramatic change of temperature gradients on the air-surface boundary. To obtain the heat capacity (2) as well as time constant τ_j (1) of the j-mass segment the lumped-capacity type analysis was used.

The assessment of thermal mass of the wall surrounding an enclosure – room of an administrative building, is necessary in order to evaluate time-depending thermal comfort of the enclosure [1], [2]. The thermal storage in the enclosure's wall influences indoor environment through two aspects:

(1) qualitative, by exposing as much of internal surface toward indoor air due radiant and convective load and, (2) quantitative, by increasing (decreasing) the air flow along the surface, thus by increasing (decreasing) its heat and mass transfer coefficient. Hovewer, there was some limitation on the laminar airflow regime on its bordering to the transient one determined by indoor comfort parameters. Mathematically, $Gr.Pr > \sim 10^9$ [3], i.e. excluding the turbulent flow.

2 Thermal Mass Functions

There are three dominant functions of the 'thermal mass': 1. energy storage, 2. temperature, resp. heat flux dumping, and 3. water vapor absorbent feature. Yet, considering only sensible heat changes, the 'thermal mass' is accepted as term for the overall effect of the amount of material with its thermal capacity. Within the mass can be stored a certain amount of heat, reduced heat and moisture (mass) transmissions as well as their fluctuations, resulting in more acceptable thermal conditions. An energy balance $q_{in} - q_{out} = q_{stored}$ (W) of an external wall segment shows Fig.1:

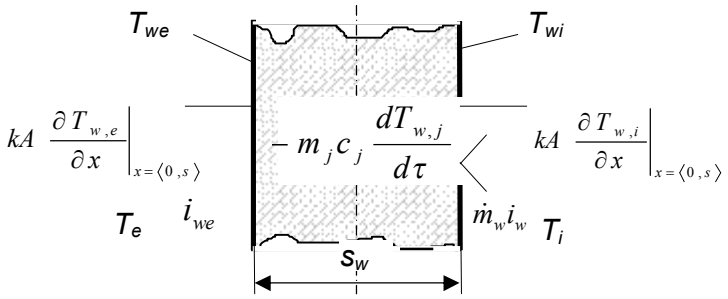

s_w - (exterior) wall thickness (m),
dS - surface area element exposed to solar radiation (m^2),
Q_s - solar radiant heat rate absorbed by surface element dS (W).

Fig.1 External wall segment - an energy balance of the wall region.

The sum term $-m_j c_j \frac{dT_{w,j}(x,\tau)}{d\tau}(\mathrm{W})$ includes a heat amount temporarily stored in the segment wall, so the problem of determining it apparently reduces on obtaining:

- specific weight (density) of the segment with its dimensions, and
- local specific heat capacity.

The mass in our study, the concrete slab vertical wall with double gypsum, refers to classical materials that have the capacity to store thermal energy for extended periods of time without phase change under which is stored and released latent heat. The sensible heat could join in very exceptional conditions the latent heat from water vapor change (ice crystals melting on the outside-facing wall surface and partially penetrating the gypsum). Depending on the material, the specific heat varies with its water content. With moisture laden air penetrating the material due a pressure difference and condensing in the wall cavity as the air temperature decreases, and it occurs alongside the temperature profile across the segment thickness of the 'storageable' segment. Because of time-variable temperature on its surface, some form of initial conditions $T_{s,j}(\tau) = f\left[T_{w,j}(\tau)\right], j = 1,2,...n(\mathrm{K})$, must be known. To respect vertical temperature profile on inner surface of the wall, adequate nodal sequence in vertical direction would form a rectangular net of nods on which the values were calculated. Further, both segments (plasters) of the wall, i.e. the ones facing exterior, resp. interior, would satisfy Bi > 0.1, as result of a dramatic change of temperature gradients on the air-surface boundary $\left.\frac{\partial T_{w,e}}{\partial x}\right|_{x=\langle 0,s\rangle}$. That allows utilize the lumped-capacity type of analysis in order to obtain the heat capacity (1) as well as time constant τ_j (2) of the *j*-mass segment. The same does not apply for anisotropic part of the j-wall and the wall segment was partitioned accordingly with spatial step Δx of the finite difference method (FDM) used in this work. Applying Laplace equation onto an isotropic homogenous part of such wall segment with different surface temperatures T_{we}, T_{wi} and boundary conditions yielded temperature profile across the region, and completed with vapor content assessment, led to the heat capacity evaluation.

3 Basic Equations and State-Variable Model

Basic relations of physical phenomena that govern the thermal energy transfer process within the slab were employed: the law of mass conservation and the first law of thermodynamics. The adjacent air layer to the wall surface where are placed the system boundaries is considered as the well-stirred system.

3.1 Heat and Mass Transfer Coefficients

Heat transfer coefficients are calculated simultaneously with sampling time and are based on relations described through several dimensionless numbers (*Nu*, *Pr*, *Re*) in literature. What follows is common practice in determining the convective heat transfer coefficients through groups of these numbers, where the dimensional analysis was employed to estimate heat transfer from vertical surfaces on the surface area x_h x b_y. x_h is the height of the wall segment and in the horizontal direction it extents to the velocity, resp. temperature profiles change adjacent to the wall surface, Fig. 2:

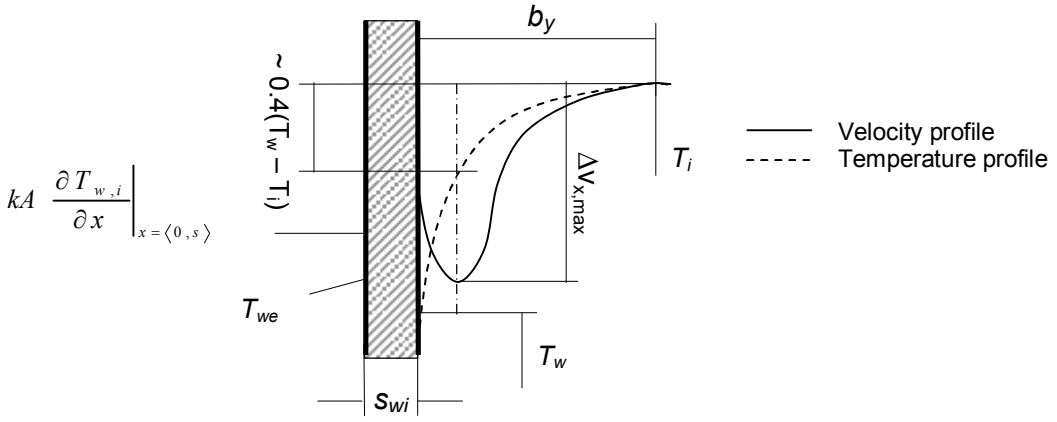

$T_{i,e}$	-	*indoor (outdoor) air temperature (K)*
T_w	-	*internal surface wall temperature (K)*
T_{we}	-	*external surface wall temperature (K)*
$\Delta v_{x,max}$	-	*maximal velocity difference (m.s^{-1})*
s_{wj}	-	*j-segment wall thickness (m).*

Fig.2 Velocity and temperature profiles of convective airflow adjacent to innermost wall segment ($T_w < T_i$).

Assuming a steady air motion without viscous dissipation, based on π-theorem, yields for 2-dimensional motion (L_x, L_y) with these relations [3], [4]:

$$Nu.\mathrm{Re}^{-1/2} = f\left(\mathrm{Pr}, \frac{Gr}{\mathrm{Re}^{5/2}}, \frac{b_y}{x_h} Gr^{*1/5}\right), \tag{3}$$

$$Nu.Gr^{*-1/5} = f\left(\mathrm{Pr}, \frac{\mathrm{Re}}{Gr^{*2/5}}, \frac{b_y}{x_h} Gr^{*1/5}\right) \tag{4}$$

The equations are valid within a laminar mixed convection motion over a vertical plate, valid in a more or less wide region of either Nusselt or Raileigh numbers, excluding the turbulent case ($Gr.Pr > \sim 10^9$), [5]. On the surfaces are unknown heat and mass (moisture) fluxes $q_w(j)$, $q_{wm}(j)$ and the velocity profiles in the area close to the walls, both resulting from complex of quantities forming Grashof, Nusselt and Prandtl numbers and can be grouped as shown in [4]. Particularly for the calculation of free convection the equation (4) yields the formula:

$$Nu.Gr^{*-1/5} = f\left(Pr, \frac{b_y}{x_h} Gr^{*1/5}\right) \quad (-) \tag{5}$$

Free convection motion characterizes the dimensionless group

$$Gr.\Pr \approx 10^8 x_h^3 (T_i - T_w) \qquad (-) \qquad (6)$$

and by a colder wall surface (assumed $T_e < T_i$) draws air downwards along the coordinate b_y. On the vertical surface wall, such flow is described through a system of equations [5] with the boundary conditions $u = 0$, $v = 0$ and $q_w(j) = -k\left(\frac{\partial T}{\partial y}\right)_{x_P=0}$ at $b_y = 0$ and $u = u_0$, $T = T_0$ at $b_y = \infty$.

Mass transfer coefficient

With the vapour permeability properties of the material deals Fick law in same manner as Fourier law incorporates the heat transfer coefficient of heat conduction problem:

$$\frac{\dot{m}_w}{A} = -D_w \frac{dC_w}{dx} \qquad (\text{kg.m}^{-2}.\text{s}^{-1}) \qquad (7)$$

where $\dot{m}_w$ – mass flux (water content) per time unit, kg.s^{-1}
A – exposed surface area, m^2
D_w – diffusion coefficient, m^2.s^{-1}
C_w – wapor concentration, kg.m^{-3}
dx – distance element perpendicular to mass transfer, m.

With introducing the mass-transfer coefficient h_{Dw} in similar manner to the heat transfer coefficient:

$$\dot{m}_w = h_{D_w} A (C_{w_2} - C_{w_1}) \qquad (\text{kg.s}^{-1}) \qquad (8)$$

where C_w is wapor concentration in two different locations (kg.m^{-3}), yields

$$h_{D_w} = \frac{D_w}{\Delta x}$$

Whereas for convection is

$$\frac{h \Delta x}{k} = f(\text{Re}, \Pr), \qquad (10)$$

or for laminar (buoancy dominated) air flow

$$\frac{h \Delta x}{k} = f(Gr, \Pr), \qquad (11)$$

there the dimensionless group completes the Schmidt number (Gilliland [6]):

$$\frac{h_{D_w} \Delta x}{D_w} = f(\text{Re}, Sc) \qquad (12)$$

with two unknown variables, namely D_w and Schmidt number $Sc = f(D_w)$. These equations were set up into a model of non-transparent part of exterior wall, Fig. 3 below. The model uses familiar thermal-electric analogy with dc-circuit (direct current) electric resistance and capacitance, equivalent to the thermal and permeance resistance, respectively:

$$R_{cv} = \frac{1}{hA} \qquad (\text{kg}^{-1}.\text{m}^{-2}.\text{s}^3.\text{K}) \qquad (14)$$

$$R_{D_w} = \frac{\Delta p}{m_{vt}} \qquad (\text{m.s}^{-1}) \qquad (15)$$

They are parameters in mathematical model which represents an equivalent thermal circuit consisting of active and passive components: thermal sources, thermal resistors and thermal capacitors. The 2-dimensional model includes the boundary conditions on both wall surfaces. Assuming the uniform vapor content distribution across the sufficiently thin sliced wall segments, the lumped parameter model incorporating both heat and mass transfer coefficients of the vertical wall illustrates Fig. 3:

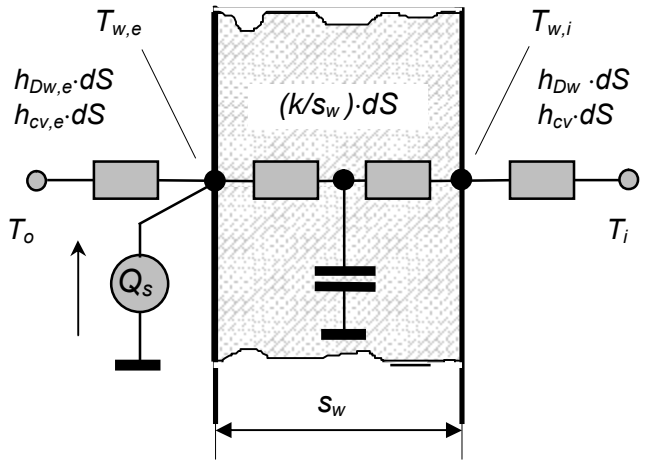

s_w	-	*wall thickness (m),*
dS	-	*surface area element exposed to solar radiation (m^2),*
Q_s	-	*solar radiant heat rate absorbed by surface element dS (W).*

Fig. 3 Analog scheme of heat transfer through exterior wall exposed to solar (short-wave) radiation.

3.2 State-Variable Model of Wall Segment

The *n*-segment wall model was set up according to the analog scheme in Fig. 3 in the MATLAB/Simulink environment. It comprises the (*n*+2)-nodal net with the innermost segment exposed to the indoor air temperature $T_w(\tau)$, resp. enthalpy $i_w(\tau)$, and on the external surface outdoor air temperature $T_{we}(\tau)$ and enthalpy $i_{we}(\tau)$, Fig. 4:

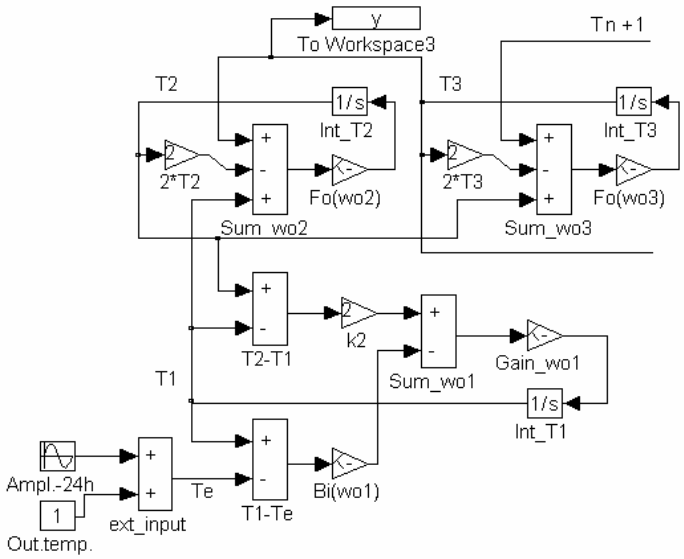

Fig. 4 Analog of exterior wall temperature distribution with convective boundary conditions (Matlab/Simulink environment).

T_{n+1}, n = 0,1,2,…,m, refers to the nodes lined up evenly in perpendicular direction to the segment wall surface's where the temperatures, as well as other qualities, are pinned. It corresponds to the values of Fourier equation in central difference scheme. The heat rates refer to thermal equilibrium served as the initial conditions in the transition processes through the wall part with surface area A exposed to various thermal excitations, Figures 5-7.

The overall time response, referring effectively to the 36.8 % of the initial temperature difference ΔT_e, yields from:

$$\tau_w = \frac{\tau_j - \tau_{td}}{n-1} \quad \text{(s)} \tag{16}$$

where τ_w denotes the overall time constant in seconds, τ_{td} is time lag (usually τ_{td} = 0 s) and n – system order. In the 6-segments composed model was estimated the value ~$2.5 \cdot 10^4$ s, and the temperature indicated quite monotonous profile, Fig. 5:

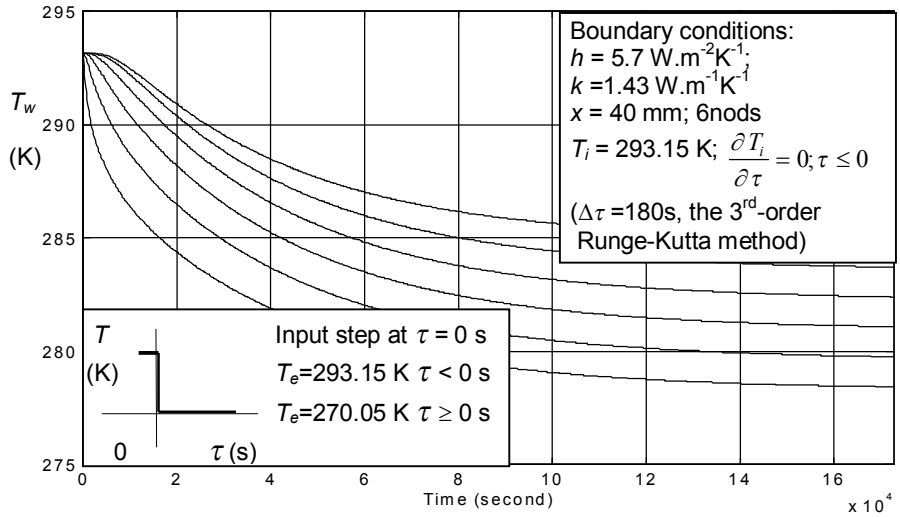

Fig. 5 Exterior wall temperature distribution profiles with convective boundary conditions; h_{cv} = 5,7 W.m^{-2}K^{-1} on both sides.

The material's relative humidity was kept constant (diffused air of 50 % relative humidity), while in the second case was used the real measured data, curve *b* in Fig. 6:

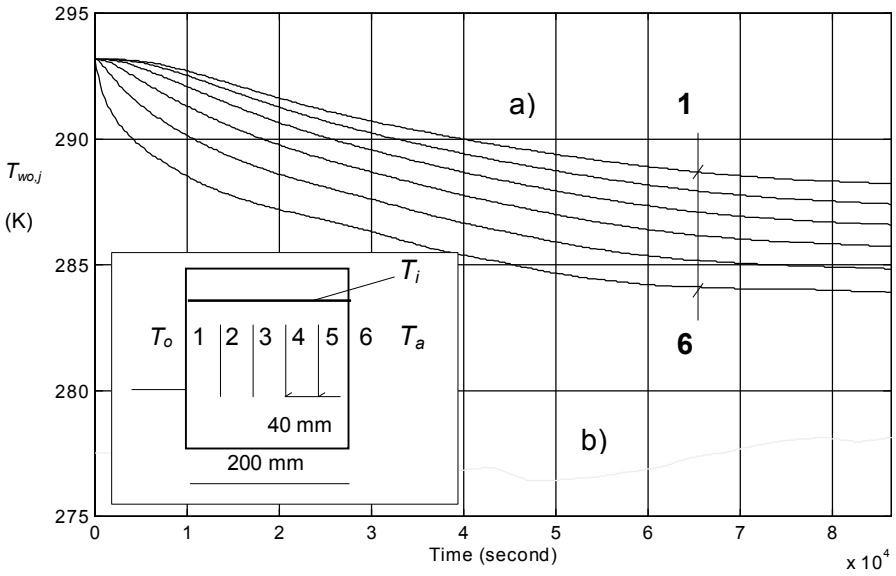

Fig. 6 Transient temperature response (a) across 200 mm-thick plain brick exterior wall suddenly exposed to ambient air temperature (b) at initial wall temperature T_i = 293 K.

For the approximation of the ambient air humidity and temperature daily swing (curve *b* at Fig.6) were found shortened time constants (Eq. (2)) over 15 % for upper end of human comfort area (30 – 70 % r.h.) corresponding to the air enthalpy content of 48 kJ.kg^{-1}. An adequate thermal capacity, $\sum_{j=1}^{6} m_j c_j = 386$ kJ.K^{-1} Eq.(1) of 20 cm thick brick wall with ratio $A_w/V_w = 0.2$ m^{-1} would be kept at value (c_1 = 839 J.kg^{-1}.K^{-1}, cases in Fig.5 and 6), and the convective heat transfer coefficient roughly followed the air enthalpy ratio:

$$\frac{i_2(\tau)}{i_1} h_{cv1} \approx h c_{cv2}(\tau) \qquad \text{(J.kg}^{-1}\text{.K}^{-1}\text{)} \qquad (17)$$

i.e. the value of 5.7 W.m^{-2}.K^{-1} would reach 6.7 W.m^{2}.K^{-1}. That represents the difference 17 % equivalent to the increase of $R_{cv} + R_{Dw}$ Eq.(14-15), it may release the heat accumulated in the fabrics proportionally shortly, under otherwise same conditions. This demonstrates Fig. 7 in which the release of accumulated amount of heat lags behind the same case in Fig. 5. The difference in the later situation caused exposing the outer wall to the nearly rectangular temperature swing (yellow curve in Fig. 7) accounts about 1.6 Kelvins in temperature difference at time of $2.5 \cdot 10^4$ s.

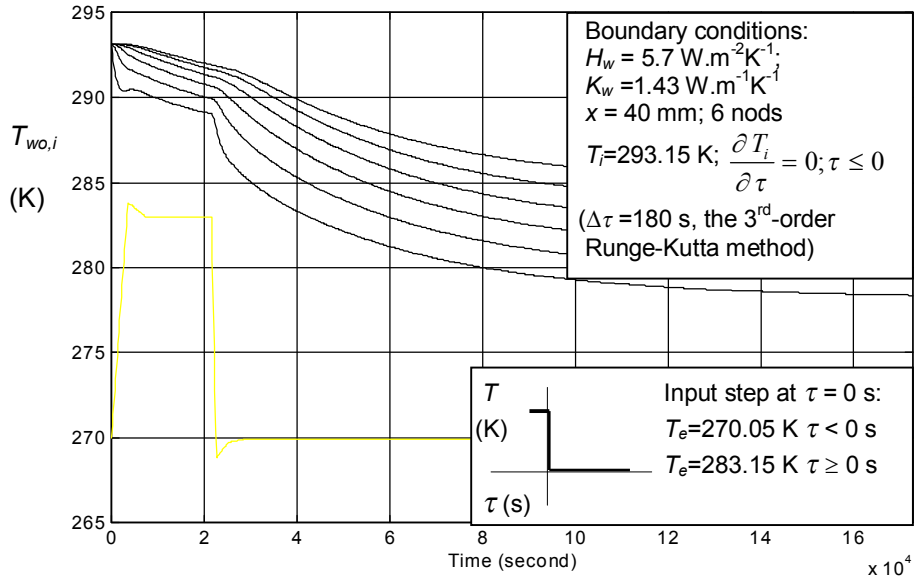

Fig. 7 Wall temperature distribution with convective boundary conditions h = 5.7 W.m^{-2}.K^{-1} on both sides exposed to nearly rectangular jump of temperature (270 K ... 283.15 K in time interval of 6 hours); the same initial and boundary conditions in the exterior wall scheme in Fig. 5.

Because the ratio of the ability to store the heat energy to the ability to conduct the heat energy could be expressed as

$$\frac{\rho c_w s_w}{\frac{k}{s_w}} \qquad \text{(s)} \qquad (18)$$

resp. with thermal diffusivity:

$$\frac{s_w^{\,2}}{a} \qquad \text{(s)} \qquad (19)$$

there could be estimated a time through the concrete slab segment in which the transient process of heat conductance would complete. With 86.5 % of the final value reached after two time constants, it reaches 95 % after three time constants. Because the time constant of the homogenous *j*-segment is from eq.(19)

$$\frac{s_{w_j}^{\ 2}}{\pi a_j} \quad \text{(s)} \tag{20}$$

the time adequate to three time constants yields approximately

$$0.3\frac{s_{w_j}^{\ 2}}{a_j} \quad \text{(s)} \tag{21}$$

The diffusivity a_j should reflect vapor penetration on each slab in horizontal direction while fluctuances within the adjacent layer of air in the vertical direction could be neglected. Instead the vertical temperature profile ($T_w=f(b_y)$), is necessary to acquire with measurement data in order to obtain convective heat transfer coefficient h_{cv}. The complementary calculation of state equation for air ($p/\rho T$ = const.) yielded assessment of the density fluctuations, thus the water content and mass-transfer coefficient, h_{Dw}. The measured values were used in a computational model of air state equation in order to fill the values of vertical temperature profile and water vapor values. The partial pressure of water vapor (air density change) along the vertical slab surface is seen in Fig. 8 on the right side:

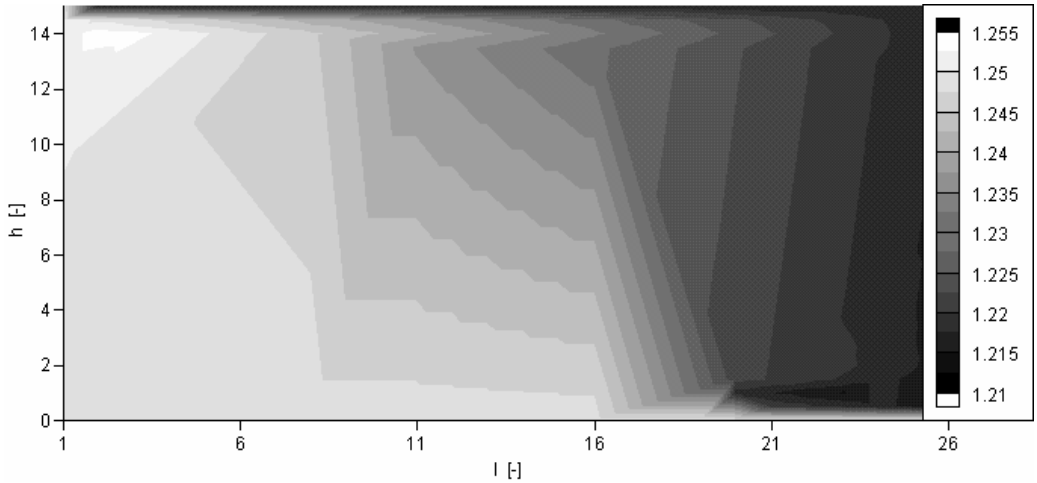

Fig.8 The air density fluctuation map in cross-cut of single-zone space with non-uniformly cooled walls (in 2D-meridian-cut, scale in kg.m^{-3}) height H =1900 mm; ACH = 0.5.

The simulation test, including periodical harmonic (sine function) disturbance (Fig.9) caused by exposing the uppermost wall surface to the external heat load, allows to estimate the wall segments thermal damping and thermal condition of reversing the temperature and permeance gradient - in which may occur dew point on construction fabrics [7], [8]. Thermal damping over the wall was characterized by a dumping coefficient

$$\nu_w = \frac{\Delta T_w}{\Delta T_{w,e}} \quad \text{(-)} \tag{22}$$

$\Delta T_{w,e}$ - temperature amplitudes difference on out-faced wall surface (K),
ΔT_w - temperature amplitudes difference on interior-faced wall surface (K)

and estimated at 0.19, the beginning of reversal permeance and temperature gradient indicates point P in Fig. 9:

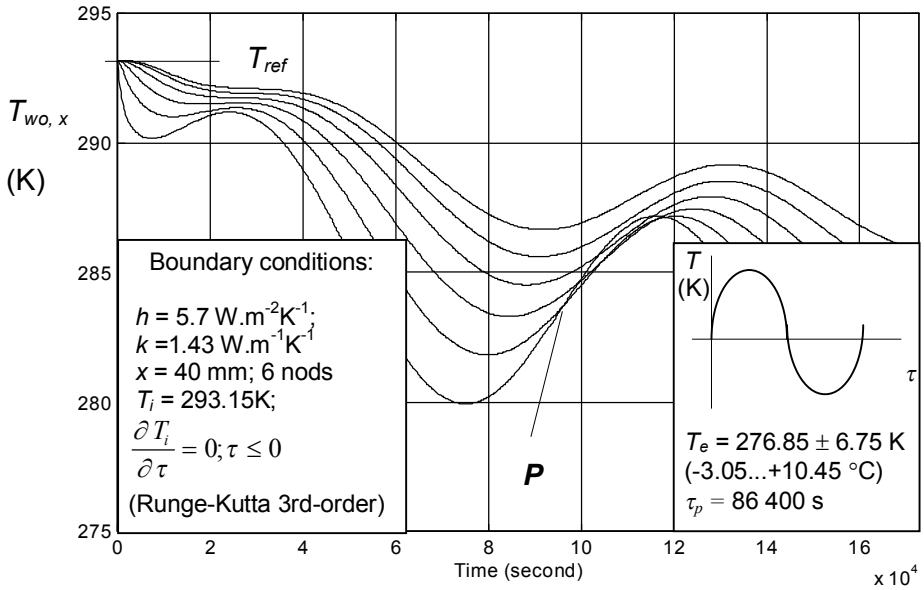

Fig.9 Wall temperature distribution with convective boundary conditions h_w = 5.7 W.m^{-2}K^{-1}. 6 nods, x = 400 mm; time step 180 s, τ_p = 86 400 s, T_i = 293.15 K; T_e= 276.85 ± 6.75 K (-3.05 ...+ 10.45°C), harmonic (sine) temperature change. Runge-Kutta 3rd-order, $Bi \cong 1.2$.

4 Solution and conclusions

The wall thermodynamic parameters were estimated in the transient period between two thermal steady and quasi-steady (real experimental data) states with several temperature and moisture varying disturbances. The concrete slab transient time in which would complete 95 % of the final value was estimated (eq.(21)) with time constant of the value ~2.5·10^4 s, Fig.6.

The wall partition perpendicular to the one-dimensional heat flux determined the model's order with boundary conditions prescribed through wall function of convective heat transfer coefficient h_{cv}, temperature T_j and mass-transfer coefficient, h_{Dw} for each wall segment's energy balance equation. Moisture diffusion in free air causes minimal vapor pressure differentials between connected places as such is minor driving force in increasing the convective heat transfer coefficient until the condensation may uccur.

The heat and mass flux reverse causes a 'cut' of wall thermal capacity, available for the interior's overall heat storage capacity. The virtual plane – *P*-points in Fig. 9 over the wall segment - moving through the wall determines a new location of the plane equation $\left.\frac{dt(\tau)}{dx}\right|_{x=x_P} = 0$. The Biot number for the *P*-plane shift from surface inside characterizes the heat storage mass capability as the time lag will become effectively shorter ($h_P \cdot (s_w - x_p) < k$).

Nomenclature:

a_i	-	thermal diffusivity of *i*-layer (m^2.s^{-1})
A_j	-	surface area of *j*-wall (m^2)
b	-	dimensionless parameter (-)
c	-	specific heat (J.kg^{-1}.K^{-1})
b_y, x_h	-	spatial dimensionless height, width (-)
h_c	-	convective heat transfer coefficient (W.m^{-2}.K^{-1})
k	-	thermal conductivity (W.m^{-1}.K^{-1})
		kinetic turbulent energy (J.kg^{-1}), (Chapter 4)
n	-	system order
p	-	air pressure (Pa)
q	-	heat flux per unit surface area (W.m^{-2})
R	-	thermal resistance (W^{-1}m^2.K)
s_w	-	wall thickness (m)

t, T	-	temperature (°C), thermodynamic temperature (K)
T_i	-	(indoor) air temperature (K)
$T_{w,j}$	-	surface temperature of inner side of j-wall (K)
T_{we}	-	surface temperature of exterior wall (K)
$T(x, \tau)$	-	temperature at time τ in distance x (K)
u	-	velocity component in x direction (m.s^{-1})
v	-	velocity component in y direction (m.s^{-1})
V	-	volume (m^3),
x, y	-	Cartesian (spatial) coordinates (m)

Greek letters

ν	(overall) dumping coefficient kinematic viscosity (m^2.s^{-1})
ρ	density (kg.m^{-3})
$\rho_i.c_i$	volumetric heat capacity of i-part (J.m^{-3}.K^{-1})
τ	time (s)

Bi, Gr,	Biot, Grashof number
Nu, Ra	Nusselt, Rayleigh number
Re	Reynolds number

References

[1] L. Hach and Y. Katoh. *Application of Quasi-Steady-State Thermodynamic Model of Conventional Heating System with Takahashi Control Method*, *IBPSA 2001*, Brazil, Proceedings 2001.

[2] C.O.R. Negrão. Integration of computational fluid dynamics with building thermal and mass flow simulation, *Energy and Buildings*, vol.27, 1998, pp.155-165.

[3] D.E. Fisher and C.O. Pedersen. *Convective Heat Transfer in Building Energy and Thermal Load Calculations*, *ASHRAE Transaction*s (1997), 103 (2) 137-148.

[4] A. Tindale. *Third-order lumped-parameter simulation method*. Building Service Engineering Research and Technology, Vol. 14 No.3, 1933, pp 87-97.

[5] F. Bauman, A. Gadgil, R. Kammerud, E. Altmayer, and M. Nansteel (1983). *Convective Heat Transfer in Buildings: Recent Research Results*, ASHRAE Transactions, 89 (1A) 215-232.

[6] E.R. Gilliland, Diffussion Coefficients in Gaseous Systems. Ind. Eng. Chem., Vol.26, p.681,1934.

[7] L. Hach, Y. Katoh. *Simulation of Thermal Balance of Non-Air Conditioned Room under Winter Conditions Using Quasi-Steady-State Simulation Model*. International Journal JSME, Vol.46, No.1, 2003.

[8] H. Recknagel, E. Sprenger, and E.-R. Schramek, Taschenbuch für Heizung und Klimatechnik, R. Oldenbourg Verlag, München, Germany, 1997.

Contact information
Dr.Eng. Lubos Hach, Ph.D., Institute of Applied Physics and Mathematics, Faculty of Chemical Engineering, Pardubice University, 532 10 Pardubice, Czech Rep., E-mail lubos.hach(a)upce.cz.